6
Cam-clay and the critical state concept

6.1 Introduction

In the last chapter we started by setting up an ideal test system (Fig. 5.4) and investigating the possible effects of a probing load-increment $(\dot{p},\dot{q})$ applied to *any* specimen within the system. By considering the power transferred between the heavy loads and the specimen within the system boundary we were able to establish two key equations, (5.14) and (5.15). These need to be recalled and repeated:
(*a*) the recoverable power per unit volume returned to the heavy loads during the *unloading* of the probe is given by

$$\frac{\dot{U}}{v} = -\left(\frac{p\dot{v}^r}{v} + q\dot{\varepsilon}^r \right) \tag{6.1}$$

and (*b*) the remainder of the loading power per unit volume (applied during the *loading* of the probe) is dissipated within the specimen

$$\frac{\dot{W}}{v} = \frac{\dot{E}}{v} - \frac{\dot{U}}{v} = \frac{p\dot{v}^p}{v} + q\dot{\varepsilon}^p \tag{6.2}$$

For the specification of Granta-gravel we assumed that there would be no recoverable strains $(\dot{v}^r \equiv \dot{\varepsilon}^r \equiv 0)$ and that the dissipated power per unit volume was $\dot{W}/v = Mp|\dot{\varepsilon}|$. With the further assumption of the existence of critical states, we had then *fully* prescribed this model material, so that the response of the loaded axial-test system to any probe was known. The behaviour of the specimen was found to have a general resemblance to the known pattern of behaviour of cohesionless granular materials.

In essence the behaviour of a specimen of Granta-gravel is typified by Fig. 6.1(a, b, c). If its specific volume is v_0, then it remains *rigid* while its stressed state (p, q) remains within the $v = v_0$ yield curve; if, and only if, a load increment is applied that would take the stressed state outside the yield curve does the specimen *yield* to another specific volume (with a marginally smaller or larger yield curve). The stable-state boundary surface in effect contains a pack of spade-shaped leaves of which the section of Fig. 6.1(a) is a typical one. Each such leaf is a section made by a plane $v = \text{constant}$, and is of identical shape but with its size determined by a scaling factor proportional to exp v.

The modification which is to be introduced in the first half of this chapter in development of a more sophisticated model[1,2], is that Cam-clay displays recoverable (but non-linear) volumetric strains. This has the effect of slightly 'curling' the leaves formed by the family of yield curves so that in plan view each appears as a curved line in Fig. 6.1(e), which is straight in the semi-logarithmic plot of Fig. 6.1(f).

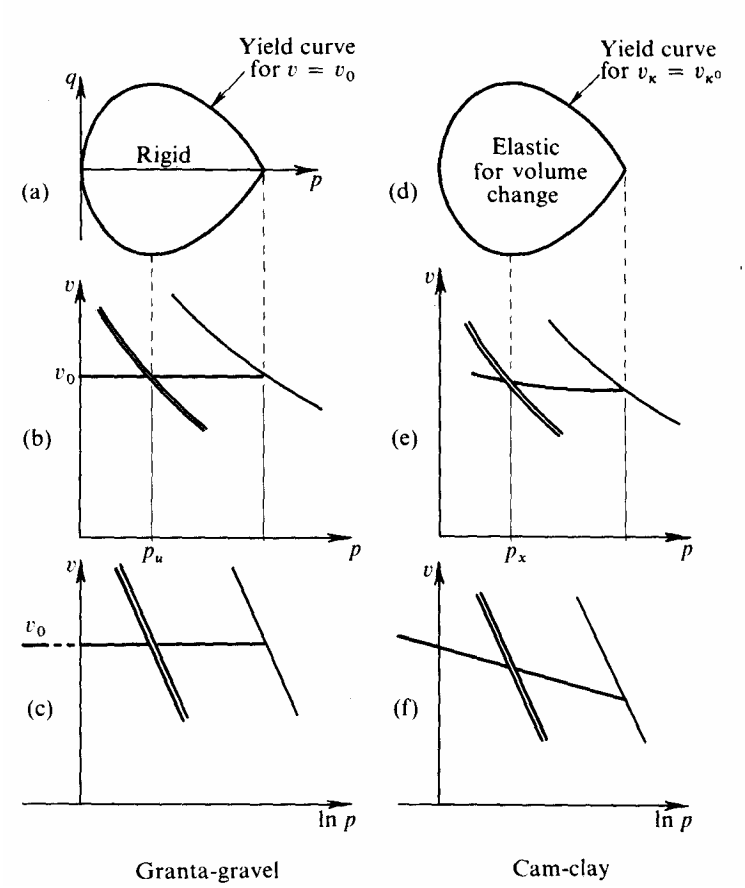

Fig. 6.1 Yield Curves for Granta-gravel and Cam-clay

Recalling the results of one-dimensional consolidation tests described in chapter 4 and in particular Fig. 4.4, we shall assume for a specimen of Cam-clay that during isotropic ($q = 0$) swelling and recompression its equilibrium states will lie on the line given by

$$v = v_0 - \kappa \ln(p/p_0) \tag{6.3}$$

in which κ is considered to be a characteristic soil constant. This line is straight in the plot of Figs. 6.1(f) and 6.2, and will be referred to as the κ-line of the specimen. It will be convenient later to denote the intercept of this κ-line with the unit pressure line p=1, by the symbol v_κ so that

$$v_\kappa = v + \kappa \ln p \tag{6.4}$$

We have seen for the Granta-gravel model the important role that lines of slope $-\lambda$ play in determining its behaviour. We shall also find it useful to denote by the symbol v_λ the intercept of the particular λ-line on which the specimen's state lies, with the unit pressure line, so that

$$v_\lambda = v + \lambda \ln p \tag{6.5}$$

As a test progresses on a yielding specimen of Cam-clay both these parameters v_κ and v_λ will vary, and they can be used instead of the more conventional parameters, v and p, for defining the state of the specimen. Each value of v_κ is associated with a particular density of random packing of the solids within a Cam-clay specimen; the packing can swell and be recompressed without change of v_κ during change of effective spherical pressure p.

We will carry our theoretical discussion of the Cam-clay model only as far as §6.7 where we show that the model can predict stress and strain in an undrained axial test. At that point we will interrupt the natural line of argument and delay the close comparison of experimental data with the theoretical predictions until chapter 7. Refined techniques are needed to obtain axial-test data of a quality that can stand up to this close scrutiny, and engineers at present get sufficient data for their designs from less refined tests. Although we expect that research studies of stress and strain will in due course lead to useful design calculations, at present most engineers only need to know soil 'strength' parameters for use in limiting-stress design calculations. We will suggest in chapter 8 that only the data of critical states of soil are fundamental to the choice of soil strength parameters. We outlined the critical state concept in general terms in §1.8, and we will return to expand this concept as a separate model in its own right in the second half of this chapter. Certain qualitative interpretations based on the critical state concept will follow, but the strong confirmation of the validity of this concept will be the closeness with which the Cam-clay model can predict the experimental data of the refined tests that are the subject of chapter 7. We do not regard this interpretation of axial-test data as an end in itself; the end of engineering research is the rationalization and improvement of engineering design. In due course the accurate calculation of soil displacements may become part of standard design procedure, but the first innovation to be made within *present* design procedure is the introduction of the critical state concept. We will see that this concept allows us to rationalize the use of index properties and unconfined compression test data in soil engineering.

6.2 Power in Cam-clay

As in §5.7 for Granta-gravel, we have to specify the four terms on the right-hand sides of eqs. (6.1) and (6.2). If we consider the application of a probe $\dot{p}$ (in the absence of any deviator stress) which takes the sample from A to B in Fig. 6.2 then the work done during loading is $p(v_a - v_b) = -p\delta v$; this is stored internally in the specimen as elastic energy which can be fully recovered as the probe is unloaded and the specimen is returned to its original state at A. The process is reversible and the amount of recoverable energy, denoted by $-p\dot{v}^r$, can be calculated from eq. (6.3) to be

$$-p\dot{v}^r = p(v_a - v_b) = \kappa\delta p = \kappa\dot{p} \tag{6.6}$$

We shall assume that Cam-clay *never displays any recoverable shear strain* so that

$$\dot{\varepsilon}^r \equiv 0 \tag{6.7}$$

Combining these, the recoverable power per unit volume

$$\frac{\dot{U}}{v} = -\left(\frac{p\dot{v}^r}{v} + q\dot{\varepsilon}^r\right) = +\frac{\kappa\dot{p}}{v} \tag{6.8}$$

We shall also assume, exactly as before, that the frictional work is given by

$$\frac{\dot{W}}{v} = Mp|\dot{\varepsilon}| > 0 \tag{6.9}$$

and so we can write

$$\frac{p\dot{v}}{v} + q\dot{\varepsilon} - \frac{\kappa\dot{p}}{v} = \frac{\dot{E}}{v} - \frac{\dot{U}}{v} = \frac{\dot{W}}{v} = Mp|\dot{\varepsilon}| \tag{6.10}$$

or (for unit volume) *loading power* less *stored energy* equals *frictional loss.*

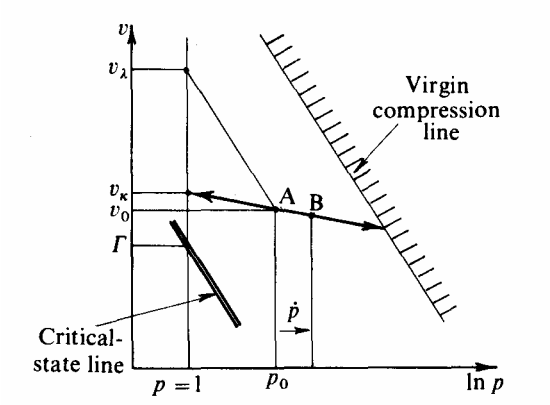

Fig. 6.2 Elastic Change of State

6.3 Plastic Volume Change

Let us suppose we have a specimen in a state of stress on the verge of yield, represented by point D in Fig. 6.3. We apply a loading increment $(\dot{p},\dot{q})$ which causes it to *yield* to state E, and on removal of the load-increment which completes the probing cycle it is left in state F having experienced permanent volumetric and shear strains. Because we have applied a full probing cycle the state of *stress* of the specimen is the same at F as at D, so these points have the same ordinate $p_f = p_d$. Because of our assumptions that Cam-clay exhibits no recoverable shear strain, and that its recoverable volumetric strain occurs *along* a κ-line, the points E and F must lie on the same κ-line, and have the same value of v_κ.

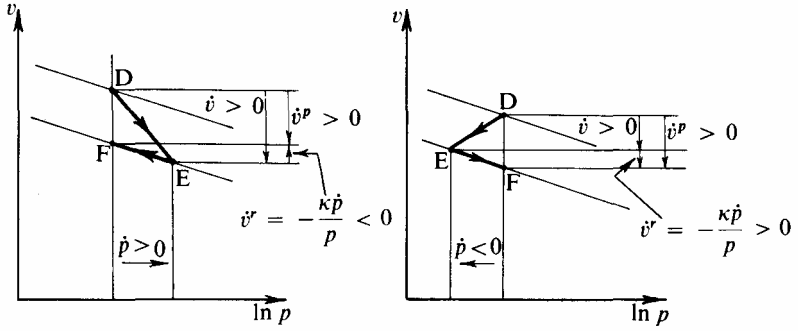

(a) 'Positive' probe ($\dot{p} > 0$) (b) 'Negative' probe ($\dot{p} < 0$)

Fig. 6.3 Plastic Volume Change during Yield

One of the unfortunate consequences of our original sign convention (compression taken as positive) is now apparent, and to avoid difficulty later the position is set out in some detail. In Fig. 6.3(a) and (b) two situations are considered, one with a probe with $\dot{p} > 0$ and the other with $\dot{p} < 0$. Remembering our sign convention, and since strain-increments must be treated as vector quantities, we have for both cases

Total volumetric strain	$\dot{v} = -(v_e - v_d)$
Recoverable volumetric strain	$\dot{v}^r = -(v_f - v_e) = -\dfrac{\kappa\dot{p}}{p}$
Resulting Plastic volumetric strain	$\dot{v}^p = -(v_f - v_d)$

Adding, and noting that $(v_f - v_d)$ is also the permanent change of v_κ experienced by the specimen, we have

$$-\delta v_\kappa = \dot{v}_\kappa = \dot{v}^p = \dot{v} + \dot{v}^r = \dot{v} - \frac{\kappa \dot{p}}{p} \tag{6.11}$$

which can be derived directly from eq. (6.4), defining v_κ.

It is important for us to appreciate that yield of the specimen has permanently moved its state from one κ-line with associated yield curve to another κ-line having a different yield curve: it is the *shift* of κ-line, measured as $\dot{v}_\kappa$, that always represents the plastic volume change $\dot{v}^p$ and governs the amount of distortion that occurs (cf. eq. (6.13) to follow).

6.4 Critical States and Yielding of Cam-clay

So far the specification of Cam-clay is

$$\dot{\varepsilon}^r \equiv 0 \qquad \dot{\varepsilon} \equiv \dot{\varepsilon}^p \qquad \dot{v}^r = \frac{\kappa \dot{p}}{p} \qquad \dot{v}^p = \dot{v}_\kappa$$

$$\frac{p\dot{v}}{v} + q\dot{\varepsilon} - \frac{\kappa \dot{p}}{v} = Mp|\dot{\varepsilon}| \qquad (\dot{\varepsilon} \neq 0) \tag{6.10 bis}$$

with the stability criterion becoming

$$\dot{p}\frac{\dot{v}^p}{v} + \dot{q}\dot{\varepsilon} \geq 0 \tag{6.12}$$

Comparison with eq. (5.19) and (5.20) confirms that Granta-gravel is merely a special case of Cam-clay when $\kappa = 0$. This distinction between the two model materials is the only one to be made; and we shall now examine the behaviour of Cam-clay in exactly the same way as the procedure of chapter 5.

Re-writing eq. (6.10) and using (6.11)

$$\frac{p\dot{v}_\kappa}{v} = \frac{p\dot{v}}{v} - \frac{\kappa \dot{p}}{v} = Mp|\dot{\varepsilon}| - q\dot{\varepsilon} \tag{6.13}$$

For the case of length reduction, $\dot{\varepsilon} > 0$, we have

$$\frac{\dot{v}_\kappa}{v\dot{\varepsilon}} = M - \frac{q}{p} \tag{6.14a}$$

and for radius reduction, $\dot{\varepsilon} < 0$,

$$\frac{\dot{v}_\kappa}{v\dot{\varepsilon}} = -M - \frac{q}{p} \tag{6.14b}$$

As a consequence we distinguish between specimens:

(a) those that are weak at yield when $(|q|/p) < M$ and $\dot{v}_\kappa = -\delta v_\kappa > 0$,

(b) those that are strong at yield when $(|q|/p) > M$ and $\dot{v}_\kappa = -\delta v_\kappa < 0$; and

(c) those that are at the critical states given by

$$|q| = Mp \tag{6.15}$$

and

$$v = \Gamma - \lambda \ln p \tag{6.16}$$

6.5 Yield Curves and Stable-state Boundary Surface

Let us consider a particular specimen of Cam-clay in equilibrium in the stressed state $\mathrm{I} \equiv (p_i, v_i, q_i)$ in Fig. 6.4, so that the relevant value of $v_\kappa = v_i + \kappa \ln p_i = v_{\kappa i}$ say. As before, we shall expect there to be a yield curve, expressible as a function of p and q, which is a boundary to all permissible states of stress that this specimen can sustain *without yielding.* In general, a small probe $(\dot{p}, \dot{q})$ will take the state of the specimen to some neighbouring point within the yield curve such as J; its effect will be to cause no shear strain $(\dot{\varepsilon} = 0)$, but a volumetric strain $\dot{v}$ which is *wholly recoverable,* and of sufficient magnitude to keep the specimen on the same κ-line, so that

$$\dot{v}_\kappa = \dot{v}^p = 0; \qquad \dot{v} = -\dot{v}^r = +\frac{\kappa \dot{p}}{p}$$

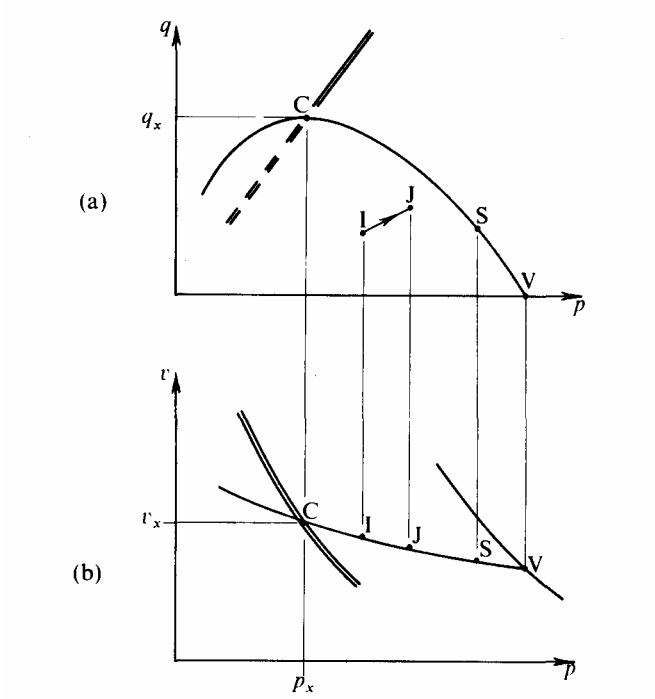

Fig. 6.4 Yield Curve for Specimen of Cam-clay

and

$$v_{\kappa i} = v_{\kappa j} = v_j + \kappa \ln p_j = (v_i - \dot{v}) + \kappa \ln(p_i + \dot{p})$$

All states *within* the yield curve are accessible to the specimen, with it displaying a rigid response to any change of shear stress q, and a (non-linear) elastic response to any change of effective spherical pressure p, so as to keep the value of v_κ constant. Probes which cross the yield curve cause the specimen to yield and experience a change of v_κ, so that it will have been permanently distorted into what in effect is a new specimen of a different material with its own distinct yield curve.

Following the method of §5.10 we find that probes which cause neutral change of a specimen at state S on the yield curve, satisfy

$$\frac{\mathrm{d}q}{\mathrm{d}p} = \frac{\dot{q}}{\dot{p}} = -\left(M - \frac{q_s}{p_s}\right) \tag{5.25bis}$$

and we can integrate this to derive the complete yield curve as

$$\frac{|q|}{Mp} + \ln\left(\frac{p}{p_x}\right) = 1 \tag{6.17}$$

In chapter 5 (p_u, q_u) were used as coordinates of the critical state on any particular yield curve, which was *planar* and therefore an *undrained* section of the state boundary surface. For Cam-clay the yield curves are no longer planar and to avoid later confusion the relevant critical state will be denoted by (p_x, q_x)—as in Fig. 6.1— and (p_u, q_u) will be reserved for the undrained section. The yield curve is only completely described in (*p*, *v*, *q*) space by means of the additional relationship

$$v_\kappa = v + \kappa \ln p = \text{constant} \tag{6.18}$$

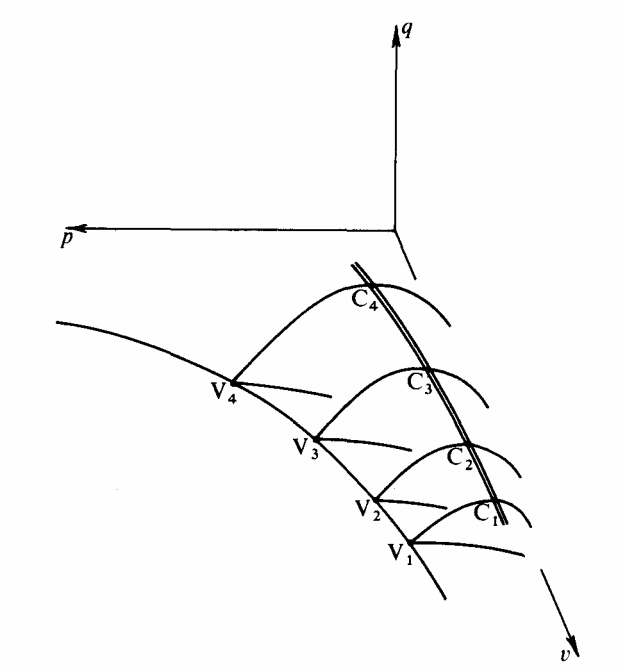

Fig. 6.5 Upper Half of State Boundary Surface for Cam-clay

The critical state point (p_x, q_x) for this one yield curve is given by the intersection of the κ-line and critical curve in Fig. 6.4(b) so that

$$\left.\begin{aligned} v + \kappa \ln p &= v_x + \kappa \ln p_x \\ \text{and} \qquad v_x &= \Gamma - \lambda \ln p_x \end{aligned}\right\}$$

Eliminating p_x and v_x from this pair of equations and eq. (6.17) we get

$$|q| = \frac{Mp}{\lambda - \kappa}(\Gamma + \lambda - \kappa - v - \lambda \ln p) \tag{6.19}$$

as the equation of the stable-state boundary surface sketched in Fig. 6.5. As a check, if we put κ=0 it must reduce to eq. (5.30) for the Granta-gravel stable-state boundary surface. Continuing the argument, as in §5.12, we find that specimens looser or wetter than critical $(v_\lambda = v + \lambda \ln p > \Gamma;$ see Fig. 6.2) will exhibit stable yielding and harden, and specimens denser or dryer than critical $(v_\lambda < \Gamma)$ will exhibit unstable yielding and soften: Fig. 5.18 will also serve for Cam-clay except that in plan view in Fig. 5.18(b) the yield curve should now appear curved being coincident with a κ-line.

6.6 Compression of Cam-clay

If we consider a set of specimens all at the same ratio $\eta = (q/p) > 0$ at yield, we find from eq. (6.19) that their states must all be on the line:

$$v_\lambda = v + \lambda \ln p = (\lambda - \kappa)\left(1 - \frac{\eta}{M}\right) + \Gamma = \text{constant} \tag{6.20}$$

This is illustrated in Fig. 6.6 where each curve given by v_λ = constant corresponds to the set of specimens with one fixed value of η and vice versa. This curve becomes a straight line in the semi-logarithmic plot of Fig. 6.6(c), which is *parallel* to the line of critical states and offset from it by a distance $(v_\lambda - \Gamma) = (\lambda - \kappa)\{a - (\eta/M)\}$ measured parallel to the v-axis.

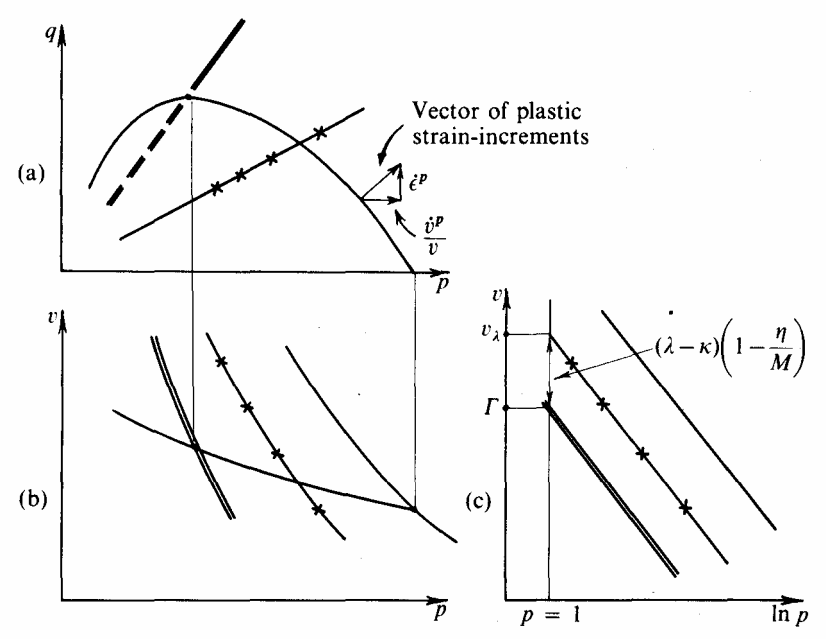

Fig. 6.6 Set of Specimens Yielding at Same Stress Ratio

If we choose to make one of this set of specimens yield continuously under a succession of load-increments chosen so that

$$\frac{\dot{q}}{\dot{p}} = \frac{q}{p} = \eta = \text{constant} > 0 \tag{6.21}$$

then its state point will progress along this line (given by eqs. (6.20) and (6.21)). As this specimen yields, the ratio of volumetric strain to shear strain is governed by eq. (6.13) for the case $\dot{\varepsilon} > 0$, i.e.,

$$\frac{p\dot{v}}{v} - \frac{\kappa\dot{p}}{v} = (Mp - q)\dot{\varepsilon} \tag{6.22}$$

but from eq. (6.20)

$$\dot{v} = -\delta v = +\frac{\lambda \delta p}{p} = \frac{\lambda \dot{p}}{p}$$

so substituting for $\dot{p}$, we get

$$\frac{\dot{v}}{v}\left(1 - \frac{\kappa}{\lambda}\right) = (M - \eta)\dot{\varepsilon} \tag{6.23}$$

For convenience we shall denote $\{(1-(\kappa/\lambda)\}$ by Λ, so that it is another soil constant (but not an independent one). Re-writing this in terms of the principal strain-increments $\dot{\varepsilon}_l$ and $\dot{\varepsilon}_r$ we have

$$\Lambda(\dot{\varepsilon}_l + 2\dot{\varepsilon}_r) = (M-\eta)\tfrac{2}{3}(\dot{\varepsilon}_l - \dot{\varepsilon}_r), \qquad (\dot{\varepsilon}_l > \dot{\varepsilon}_r)$$

or for length reduction

$$\frac{\dot{\varepsilon}_l}{\dot{\varepsilon}_r} = \frac{2M - 2\eta + 6\Lambda}{2M - 2\eta - 3\Lambda} \tag{6.24}$$

Similarly, for a case of radius reduction when $\eta < 0, \dot{\varepsilon} < 0, \dot{\varepsilon}_l < \dot{\varepsilon}_r$, we obtain

$$\frac{\dot{\varepsilon}_l}{\dot{\varepsilon}_r} = \frac{2M + 2\eta - 6\Lambda}{2M + 2\eta + 3\Lambda} \tag{6.25}$$

The values of these ratios depend on the material constants and on η, but for a given ratio of principal stresses Cam-clay undergoes compression with successive principal strain-increments in constant ratio.

One special case is isotropic compression in the axial-test apparatus where the *imposed* boundary conditions are that $q \equiv 0$, i.e., $\eta \equiv 0$. From experience we expect there not to be any distortion (in the absence of deviator stress) so that the loading increments of $\dot{p}$ would only produce volumetric strain. Unfortunately, the mathematical prescription of Cam-clay produces uncertainty for this particular case; if we take the limit as $\eta \to 0$ for eqs. (6.24) and (6.25) we have

$$\left.\begin{aligned} \frac{\dot{\varepsilon}_l}{\dot{\varepsilon}_r} &\to \frac{2M + 6\Lambda}{2M - 3\Lambda} && \text{for } \dot{\varepsilon}_l > \dot{\varepsilon}_r \\ \frac{\dot{\varepsilon}_l}{\dot{\varepsilon}_r} &\to \frac{2M - 6\Lambda}{2M + 3\Lambda} && \text{for } \dot{\varepsilon}_l < \dot{\varepsilon}_r \end{aligned}\right\}$$

These limiting ratios do not allow the possibility that $\dot{\varepsilon}_l$ is equal to 4 (unless $\kappa = \lambda$ which is unacceptable). This is an example of a difficulty met in the theory of plasticity when a yield curve has a corner: there are always two alternative limiting plastic strain increment vectors, depending on the direction from which the corner was approached. It is usual to associate any plastic strain- increment vector that lies *between* these two limiting vectors with yielding *at* the state of stress at the corner. Amongst these permissible vectors is the one *along* the *p-axis* corresponding to $\dot{\varepsilon}^p = 0$, i.e., $\dot{\varepsilon}_l = \dot{\varepsilon}_r$.

Although there is uncertainty about distortions, the volumetric strains associated with this condition are directly given by eq. (6.20) from which $v = \lambda\dot{p}/p$. These Cam-clay specimens are metastable; yielding under *any* increment $\dot{p} > 0$ of effective spherical pressure, they exist in a state of isotropic compression at the corners of successive yield curves. It has been usual to call real soil specimens 'normally consolidated' under these conditions: such specimens of Cam-clay are in a very special and abnormal condition and (because the term 'consolidation' is reserved for the transient process of drainage) we prefer to call them *virgin compressed.*

Above, we chose a particular stress ratio η and then calculated the associated vector of plastic strain-increments. We could equally well have chosen a particular combination of strain-increments and then located a point on the Cam-clay yield curve where that given vector is normal to the curve. This method is necessary for the analysis of one-dimensional compression in the consolidometer where the boundary conditions imposed are such that $\dot{\varepsilon}_r \equiv 0$ and hence $\dot{v}/v\dot{\varepsilon} = 3/2$. From eq. (6.23) we find that $\eta = M - \frac{3}{2}\Lambda$ and this determines

one point on the curve if $M > \frac{3}{2}\Lambda$. However, if $M \le \frac{3}{2}\Lambda$, then we must associate this particular strain-increment vector with yielding at the corner where $\eta = 0$. Thus, if the coefficient of earth pressure 'at rest' is defined as $K_0 = \sigma'_r / \sigma'_l$, we have

$$K_0 = \frac{\sigma'_r}{\sigma'_l} = \frac{3-\eta}{3+2\eta} = \begin{cases} 1 & for \quad M \le \frac{3}{2}\Lambda \\ \dfrac{6-2M+3\Lambda}{6+4M-6\Lambda} < 1 & for \quad M > \frac{3}{2}\Lambda \end{cases} \tag{6.26}$$

Values of K_0 predicted by eq. (6.26) are higher than those measured in practice. In recent research,[3] to resolve this difficulty, a modified form of the Cam-clay model has been suggested.

6.7 Undrained Tests on Cam-clay

We have now reached a stage where we can imagine an undrained test on a specimen of Cam-clay, and justify its existence as a model and its superiority over Granta-gravel. Let us consider a specimen virgin compressed in an initial state $(p_0, v_0, q = 0)$ represented by point V in Fig. 6.7 so that $v_{\lambda_0} = v_0 + \lambda \ln p_0 = \Gamma + \lambda - \kappa$. This is already on the yield curve (at the vertex) corresponding to its particular structural packing, v_{κ_0}, so that as soon as any load-increment is applied yielding will occur at once.

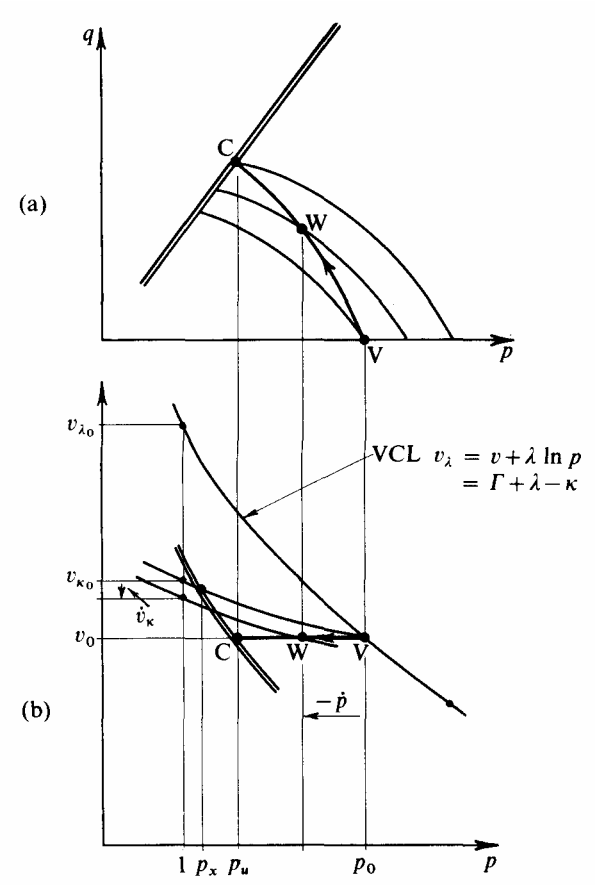

Fig. 6.7 Undrained Test Path for Virgin Compressed Specimen of Cam-clay

The volumetric strains must satisfy eq. (6.11) viz. $\dot{v}_\kappa = \dot{v}^p = \dot{v} - (\kappa \dot{p}/p)$ and also the added restriction $\dot{v} \equiv 0$ imposed by the requirement that our test should be undrained.

Hence, as the point representing the state of the sample moves across the stable-state boundary surface from V to a neighbouring point W, the shift $\dot{v}_\kappa$ of κ-line must be exactly matched by a reduction of effective spherical pressure of amount $-\kappa\dot{p}/p$. This compensating change of effective spherical pressure will be brought about by an increase of pore-pressure, as was discussed in §5.15.

This process will continue with the test path moving obliquely through successive yield curves until the critical state (p_u, v_0, q_u) is reached at C. The equation of the test path is obtained by putting $v = v_0 = \Gamma + \lambda - \kappa - \lambda \ln p_0$ into eq. (6.19) of the stable-state boundary surface

$$|q| = \frac{Mp}{\lambda - \kappa}(\lambda \ln p_0 - \lambda \ln p) = \frac{Mp}{\Lambda} \ln\left(\frac{p_0}{p}\right) \tag{6.27}$$

This is related to the initial effective spherical pressure p_0 and can be alternatively expressed in terms of the critical effective spherical pressure p_u, since

$$\left.\begin{aligned} v_0 + \lambda \ln p_u &= \Gamma \\ \text{and} \quad v_0 + \lambda \ln p_0 &= \Gamma + \lambda - \kappa \end{aligned}\right\} \text{ or } \ln\left(\frac{p_0}{p_u}\right) = \Lambda,$$

$$\text{i.e.,} \qquad |q| = \frac{Mp}{\Lambda}\left\{\Lambda - \ln\left(\frac{p}{p_u}\right)\right\} \tag{6.28}$$

Either of these equations represents the test path in the plot of Fig. 6.7(a).

The rate of distortional strain experienced along the test path comes directly from eq. (6.13) with

$$\left.\begin{aligned} \dot{v} &= 0 \\ v &\equiv v_0 \end{aligned}\right\}, \qquad \text{i.e.,} \qquad -\frac{\kappa\dot{p}}{v_0} = Mp|\dot{\varepsilon}| - q\dot{\varepsilon}$$

Choosing the conventional case of length reduction $\dot{\varepsilon} > 0, q > 0$ this becomes

$$\frac{-\dot{p}}{p\dot{\varepsilon}} = \frac{Mv_0}{\kappa}\left(1 - \frac{q}{Mp}\right) = \frac{Mv_0}{\kappa\Lambda} \ln\left(\frac{p}{p_u}\right) \tag{6.29}$$

Integrating

$$\frac{Mv_0}{\kappa\Lambda}\varepsilon = \int \frac{-\mathrm{d}p}{p \ln(p/p_u)} = -\ln\left[\ln\left(\frac{p}{p_u}\right)\right] + \text{const.}$$

and measuring ε from the beginning of the test we have

$$\ln\left(\frac{p}{p_u}\right) = \Lambda \exp\left(-\frac{Mv_0}{\kappa\Lambda}\varepsilon\right) \tag{6.30}$$

Substituting back into equation (6.28) we obtain

$$\frac{q}{Mp} = 1 - \exp\left(-\frac{Mv_0}{\kappa\Lambda}\varepsilon\right) \tag{6.31}$$

Both of these relationships are illustrated in Fig. 6.8 and provide a complete description of an undrained test on a virgin compressed specimen of Cam-clay. Detailed comparison with experimental resuits is made in the next chapter, but reference to Fig. 5.26 for Granta-gravel shows that the introduction of recoverable volumetric strains in Cam-clay has allowed us to conduct meaningful undrained tests.

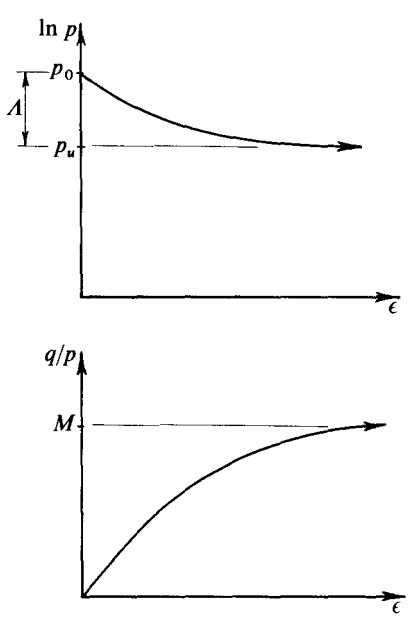

Fig. 6.8 Undrained Test Results for Virgin Compressed Specimen of Cam-clay

6.8 The Critical State Model

The critical state concept was introduced in §1.8 in general terms. We are now in a position to set up a model for critical state behaviour, postulating the existence of an ideal material that flows as a frictional fluid at constant specific volume v when, and only when, the effective spherical pressure p and axial-deviator stress q satisfy the eqs. $q = Mp$ (5.22 bis) and $v = \Gamma - \lambda \ln p$ (5.23 bis).

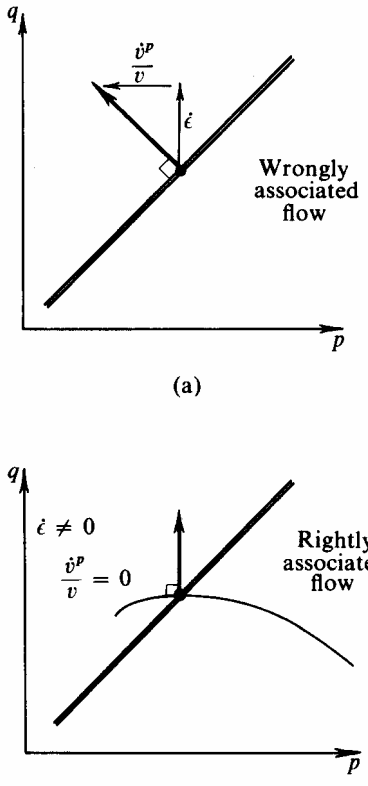

Fig. 6.9 Associated Flow for Soil at Critical State

This concept was stated in 1958 by Roscoe, Schofield and Wroth[4] in a slightly different form, but the essential ideas are unaltered. Two hypotheses are distinguished: first is the concept of *yielding* of soil through progressively severe distortion, and second is the concept of *critical states* approached after severe distortion. Two levels of difficulty are recognized in testing these hypotheses: specimens *yield* after a slight distortion when the magnitudes of parameters *(p, v, q*) as determined from mean conditions in a specimen can be expected to be accurate, but specimens only approach the *critical state* after severe distortion and (unless this distortion is a large controlled shear distortion) mean conditions in the specimen can- not be expected to define accurately a point on the critical state line.

It seems to us that the simple critical state concept has validity in relation to two separate bodies of engineering experience. *First,* it gives a simple working model that, as we will see in the remainder of this chapter, provides a rational basis for discussion of plasticity index and liquid limit and unconfined compression strength; this simple model is valid with the same accuracy as these widely used parameters. *Second,* the critical state concept forms an integral part of more sophisticated models such as Cam-clay, and as such it has validity in relation to the most highly accurate data of the best axial tests currently available. Certain criticisms[5,6] of the simple critical state concept have drawn attention to the way in which specimens 'fail' before they reach the critical state: we will discuss failure in chapter 8.

The error introduced in the early application of the associated flow rule in soil mechanics can now be cleared up. It was wrongly supposed that the critical state line in Fig. 6.9(a) was a yield curve to which a normal vector could be drawn in the manner of §2.10: such a vector would predict very large volumetric dilation rates $\dot{v}^p / v\dot{\varepsilon} = M$. However, we have seen that the set of points that lie along the critical state line are *not* on one yield curve: through each critical state point we can draw a segment of a yield curve parallel to the *p*-axis in Fig. 6.9(b). Hence it is correct to associate a flow vector which has $\dot{v}^p = 0$ with each of the critical states. At any critical state very large distortion can occur without change of state and it is certainly not possible to regard the move from one critical state to an adjacent critical state as only a neutral change: the critical state curve is not a yield curve.

6.9 Plastic Compressibility and the Index Tests

If we have a simple laboratory with only a water supply, a drying oven, a balance and a simple indentation test equipment (such as the falling cone test widely used in Scandinavia), we can find a value of λ for a silty clay soil. We mix the soil with water and remould it into a soft paste: we continually remould the soil and as it dries in the air it becomes increasingly strong. There will be a surface tension in the water of the menisci in the wet soil surface that naturally compresses the effective soil structure as water evaporates. As long as the soil is continually being remoulded it must remain at the critical state. We use the simple indentation test equipment to give us an estimate of the 'strength' of the soil, and we prepare two specimens A and B such that their strengths q_a and q_b, are in the ratio

$$\frac{q_b}{q_a} = 100$$

within the accuracy of our simple test equipment.

While we are handling the specimens in the air the external *total* stress is small, but the water tensions generate effective spherical pressures p_a and p_b. We can not measure the

effective spherical pressure directly, but from the critical state model we know in Fig. 6.10(a) that

$$q_a = Mp_a \qquad \text{and} \qquad q_b = Mp_b$$

so that

$$\frac{q_b}{q_a} = 100 = \frac{p_b}{p_a}$$

and the ratio of indentation test strengths gives an indirect measure of the increase in effective spherical pressure that has occurred during the drying out of the soil specimens.

We find the water contents (expressing them as ratios and not percentages) of each specimen w_a and w_b using the drying oven and balance. Assuming that the specific gravity G_s of the soil solids is approximately 2.7 we have

$$v_a - v_b = G_s(w_a - w_b) \cong 2.7(w_a - w_b)$$

From the critical state model we have from Fig. 6.10(b) and eq. (5.23 bis)

$$v_a + \lambda \ln p_a = \Gamma = v_b + \lambda \ln p_b$$

Hence $$2.7(w_a - w_b) \cong v_a - v_b = \lambda \ln \frac{p_b}{p_a} = \lambda \ln 100 = 4.6\lambda,$$

i.e., $$\lambda \cong 0.585(w_a - w_b) \qquad (6.32)$$

so that we can readily calculate λ from the measured water contents. The loss of water content that corresponds to a certain proportional increase in strength is a measure of the plastic compressibility of the soil.

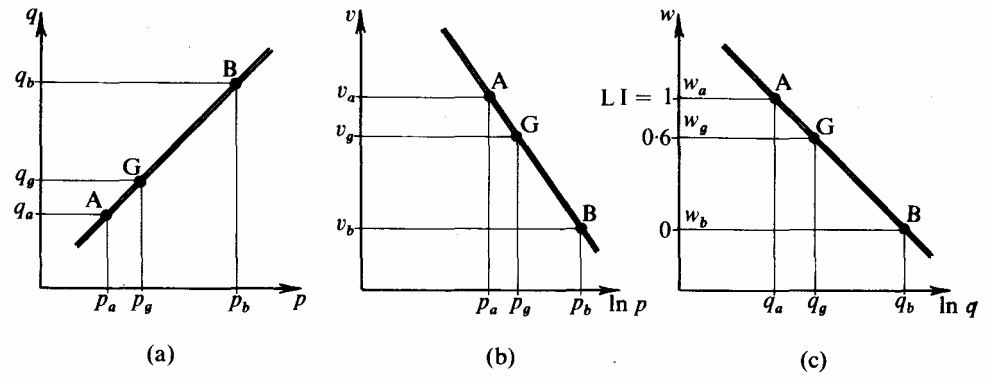

Fig. 6.10 Critical State Line and Index Tests

If we prepare further specimens that have intermediate values of indentation test strength, then we will expect in Fig. 6.10(c) to be able to plot general points such as G on the straight line AB on the graph of water content against 'strength' (on a logarithmic scale). If we arbitrarily choose to define the state of the soil at A as *liquid* and the state of the soil at B as *plastic* then we can define a *liquidity index* $=(w_g\text{-}w_b)/(w_a\text{-}w_b)$ which gauges the position of the specimen G in the range between B and A. We can then add a second set of numbers to the left of Fig. 6.10(c), giving zero liquidity to B, about 0.6 liquidity to G (in the particular case shown) and unit liquidity to A. It is a direct consequence of the critical state model that a plot of this liquidity index against the logarithm of strength should give a straight line.

In §1.3 we discussed the widely used and well-respected index tests of soil engineering. In the liquid limit test it seems that high decelerations cause a miniature slope-failure in the banks of the groove of Fig. 1.3: the conditions of the test standardize

this failure, and we might expect that it corresponds with some fixed value of shear strength q.

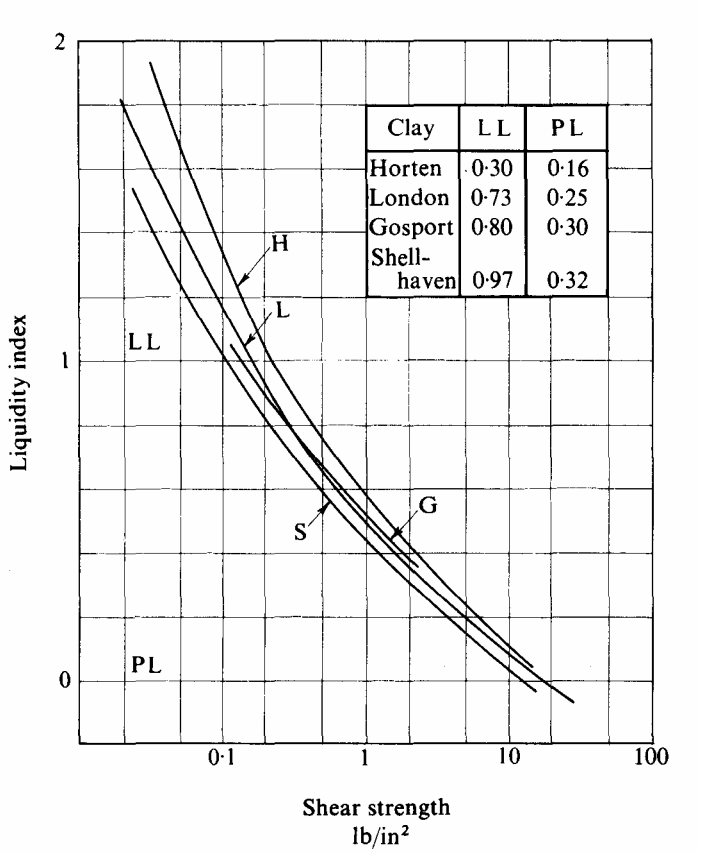

Fig. 6.11 Relation between Liquidity Index and Shear Strength of Remoulded Clays (After Skempton & Northey)

In the plastic limit test the 'crumbling' of soil implies a tensile failure, rather like the split-cylinder[7] or Brazil test of concrete cylinders: it would not seem that conditions in this test could be associated with failure at a specific strength or pressure.

However, in a paper by Skempton and Northey[8] experimental results with four different clays give similar variation of strength with liquidity index as shown in Fig. 6.11. From these data it appears that the liquid limit and plastic limit do correspond approximately to fixed strengths which are in the proposed ratio of 1:100, and so we can reasonably adopt A as the liquid limit and B as the plastic limit.

The measured difference of water contents $(w_a - w_b)$ then corresponds to *the plasticity index* of real silty clay, and we can generalize eq. (6.32) as

$$\lambda \cong 0.585\text{PI} \cong 0.217\Delta v_{\text{PI}} \tag{6.33}$$

where Δv_{PI} denotes the plasticity index expressed as a change of specific volume instead of the conventional change of water content $\Delta w\{= (\Delta v)/(G_s)\}$. Similarly, it will be useful to denote the liquid and plastic limits as v_{LL} and v_{PL}. (In eq. (6.33) and subsequent equations, PI, LL and PL are expressed as ratios and not percentages of water content.)

In Fig. 6.12 the critical state lines for several soils are displayed, and these have been drawn from the experimental data assembled in Table 6.1. Each line has been continued as an imaginary straight dashed line[9] beyond the range of experimental data at present available; this extrapolation is clearly unlikely to be justified experimentally because besides any question of fracture and degradation of the soil particles under such

high pressures, the lines cannot cross and must be asymptotic to the line $v = 1$ which represents a specimen with zero voids.

However, this geometrical extension allows some interesting analysis to be developed since these dashed lines all pass through, or very near, the single point Ω given by $v_\Omega \cong 1.25, p_\Omega \cong 1500$ lb/in^2. In addition, the points on each critical state line corresponding to the liquid and plastic limits have been marked. Those associated with the plastic limit are all very close to the same effective spherical pressure $p = p_{PL} \cong 80$ lb/in^2. The pressures p_{LL} associated with the liquid limits show a much wider range of values but this scatter is exaggerated by the logarithmic scale.

In Fig. 6.13 these experimental observations have been idealized with all lines passing through Ω, and p_{LL} and p_{PL} assumed to have fixed values. This means that in Fig. 6.14, where the liquidity index has replaced specific volume as the ordinate, all critical state lines *coincide* to one unique straight line.

For any one critical state line in Fig. 6.13 (that is for any one soil) we have

$$v_{PL} - v_\Omega = \lambda \ln\left(\frac{\Omega}{p_{PL}}\right) \tag{6.34a}$$

$$v_{LL} - v_\Omega = \lambda \ln\left(\frac{\Omega}{p_{LL}}\right) \tag{6.34b}$$

$$\Delta v_{PI} = v_{LL} - v_{PL} = \lambda \ln\left(\frac{p_{PL}}{p_{LL}}\right) \tag{6.34c}$$

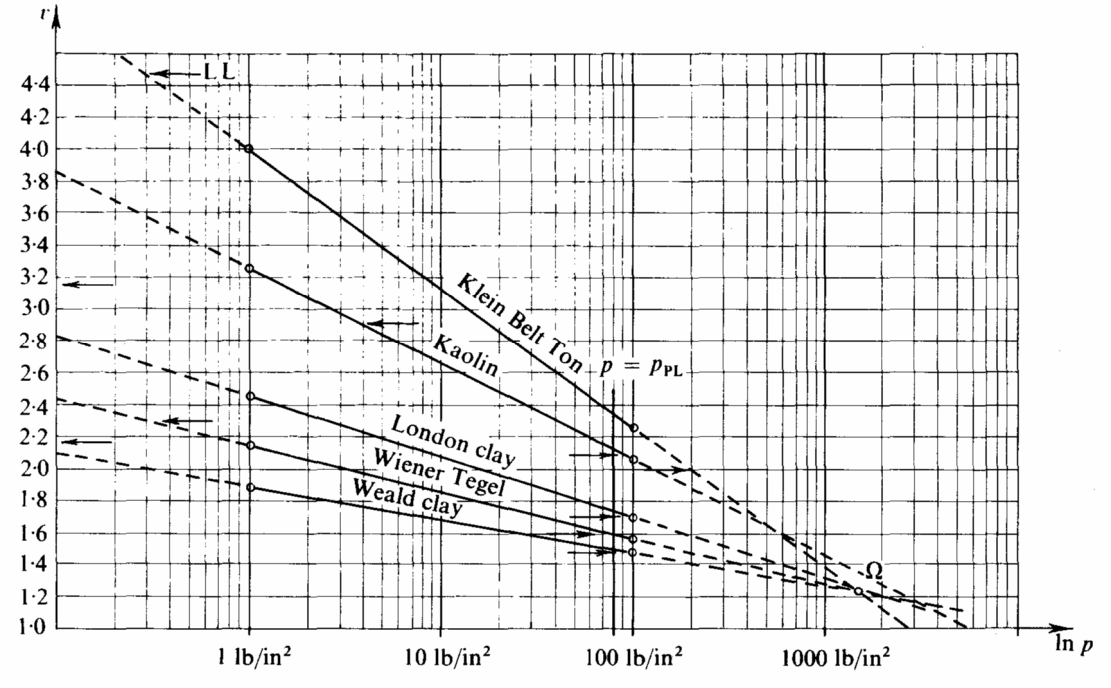

Fig. 6.12 Family of Experimental Critical State Lines

Properties		Klein Belt Ton	Wiener Tegel V	London Clay	Weald Clay	Kaolin
Critical state values	λ	0·356	0·122	0·161	0·093	0·26
	Γ	3·990	2·130	2·448	1·880	3·265
	v for $p=100$ lb/in^2	2·350	1·558	1·700	1·480	2·065
	M	0·845	1·01	0·888	0·95	1·02
Equivalent friction angle		$21\frac{3}{4}°$	$25\frac{3}{4}°$	$22\frac{1}{2}°$	$24\frac{1}{4}°$	26°
Average κ		0·184	0·026	0·062	0·035	0·05
$\Lambda=(\lambda-\kappa)/\lambda$		0·483	0·788	0·614	0·628	0·807
Liquid limit	w_{LL}	1·27	0·47	0·78	0·43	0·74
	v_{LL}	4·520	2·300	3·144	2·180	2·930
Plastic limit	w_{PL}	0·36	0·22	0·26	0·18	0·42
	v_{PL}	2·00	1·607	1·715	1·495	2·108
Plasticity index	Δw_{PI}	0·91	0·25	0·52	0·25	0·32
	Δv_{PI}	2·52	0·693	1·429	0·685	0·822
	G_s	2·77	2·76	2·75	2·75	2·61
Source of data		Hvorslev		Parry		Loudon

Table 6.1 Typical values of soil constants for a wide range of clays

Note. The critical-state values for Klein Belt Ton and Wiener Tegel V are based on results of Shearbox tests on the assumption that $\sigma'_2=\frac{1}{2}(\sigma'_1+\sigma'_3)$ at the critical state; evidence of this has been observed by Bassett, reference 11 of chapter 5.

Substituting the quoted values for Ω and p_{PL} in the first of these equations we get

$$v_{PL}-1.25=\lambda\ln\frac{1500}{80}=2.93\lambda,$$

i.e., $$\lambda=0.341(v_{PL}-1.25)\cong 0.92(PL-0.09) \qquad (6.35)$$

This predicted linear relationship is drawn as a dashed line in Fig. 6.15 where the experimental point for each soil is also plotted.

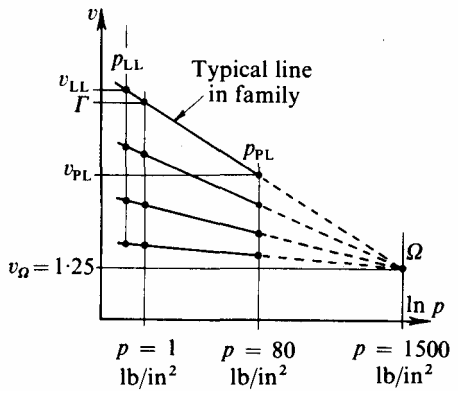

Fig. 6.13 Idealized Family of Critical State Lines

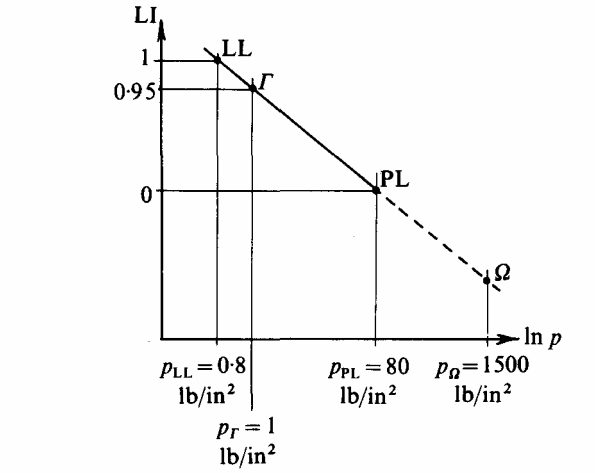

Fig. 6.14 Idealized Critical State Line

Similarly, we can predict from eq. (6.34b) the linear relationship

$$\lambda = 0.133(v_{\mathrm{LL}} - 1.25) \cong 0.36(\mathrm{LL} - 0.09) \tag{6.36}$$

on the basis that $p_{\mathrm{PL}} \cong 100 p_{\mathrm{LL}}$, so that eq. (6.34c) is identical with (6.33).

The best correlation of these predicted results with the quoted data is that between λ and the plastic limit simply because p_{PL} seems to be conveniently defined by the test conditions as approximately

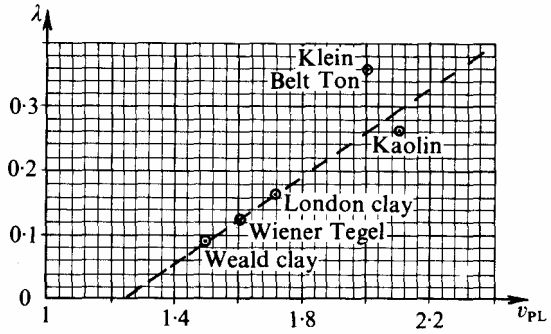

Fig. 6.15 Relationship between λ and Plastic Limit

80 lb/in^2. This suggests that the plastic limit test may be more consistent than the liquid limit test in measuring associated soil properties.

From this simple approach we can deduce two further simple relationships. The first connects plasticity index with the liquid limit; by elimination of λ from eqs. (6.33) and (6.36)

$$\mathrm{PI} \cong 1.71\lambda \cong 0.615(\mathrm{LL} - 0.09) \tag{6.37}$$

This relationship has been drawn as the heavy straight line 'B' in Casagrande's plasticity chart[10] in Fig. 6.16 and should be compared with his 'A' line

$$\mathrm{PI} \cong 0.73(\mathrm{LL} - 0.2)$$

The second relationship connects the compression index C'_c for a remoulded clay with the liquid limit. In eq. (4.1) the virgin compression curve was defined by $e = e_0 - C'_c \log_{10}(\sigma'/\sigma'_0)$, which is comparable to $v = v_0 - \lambda \ln(p/p_0)$ except that the logarithm is to the base of ten. Hence,

$$C'_c = \lambda \ln 10 = 2.303\lambda \cong 0.83(\mathrm{LL} - 0.09) \tag{6.38}$$

which compares well with Skempton's empirical relationship[11]

$$C'_c = 0.7(\mathrm{LL} - 0.1)$$

The parameter Γ was defined as the specific volume of the point on the critical state line corresponding to unit pressure which we have adopted as 1 lb/in^2. We must be careful to realize that the value of Γ for any soil will be associated with the particular unit chosen for pressure (and will change if we alter our system of units).

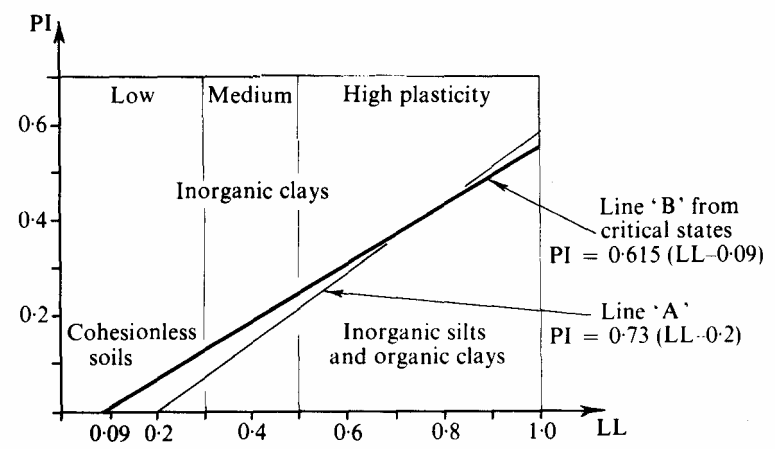

Fig. 6.16 Plasticity Chart (After Casagrande)

From the idealized situation of Fig. 6.14 we can predict that

$$\Gamma \cong v_\Omega + \lambda \ln 1500 = 1.25 + 7.3\lambda$$

which from eqs. (6.33) and (6.35) can be written in the forms

$$\Gamma \cong 1.25 + 6.7(\mathrm{PL} - 0.09) = 0.65 + 6.7\mathrm{PL}$$

$$\cong 1.25 + 4.27\mathrm{PI} \qquad (6.39)$$

At the bottom of the family of critical state lines in Fig. 6.13 we have the silty sandy soils that are almost non-plastic with low values of λ. These soils show almost no variation of critical specific volume with pressure, and it is for such soils that Casagrande first introduced[12] his original concept of a *critical void ratio* independent of pressure.

In contrast, at the top of the family of lines we have the more plastic silty clays and clays. It was for such soils that Casagrande later used[13] data of undrained axial-tests to derive a modified concept of critical 'conditions at failure' with voids ratio dependent on pressure.

In this section we have suggested various relationships between the constants of the critical state model and the index tests which are in general agreement with previous empirical findings. We also see that we could obtain a reasonably accurate value of λ from a simple apparatus such as that of the falling cone test, and can confirm this by establishing the plastic limit for the soil, which can also give us an estimate of the value of Γ.

6.10 The Unconfined Compression Strength

The critical state model is the natural basis for interpretation of the unconfined compression test. It is a simple test in which a cylindrical specimen of saturated clayey soil sustains no total radial stress $\sigma_r = 0$, and the total axial stress σ_l is rapidly increased until the specimen yields and fails. The unconfined compressive strength q_u is defined to equal the ultimate total axial stress σ_l. No attempt is made to measure pore-pressure, and no sheath is used to envelop the specimen, but the whole operation is so rapid relative to the

drainage of the specimen that it is assumed that there is no time for significant change of volume. Thus the specimen still has its *initial* specific volume v_0 when it attains its *ultimate* total axial stress $\sigma_l = q_u = 2c_u$.

We have already discussed in §6.7 the close prediction of changes of pore-pressure during the yielding of undrained specimens of Cam-clay: in the unconfined compression test no measurement is taken until the termination of yielding at what we will assume to be the critical state. So a simple prediction of the ultimate *effective* stresses can be made by introducing the initial specific volume v_0 into the equations for the critical state line

$$q = Mp \; and \qquad v_0 = \Gamma - \lambda \ln p$$

With $\sigma_r = 0$ and $\sigma_l = 2c_u$, $q = \sigma_l - \sigma_r = 2c_u$ so that

$$c_u = \frac{M}{2}\exp\left(\frac{\Gamma - v_0}{\lambda}\right) \tag{6.40}$$

This equation expresses c_u in terms of v_0, the soil constants λ, Γ, M and the same units of pressure as that used in the definition of Γ (i.e., lb/in^2). In Fig. 6.7 this is equivalent to disregarding the stress history of the specimen along the path VWC and assuming that the path merely ends at the point C.

Let us apply this result to samples of soil taken at various depths from an extensive stratum of 'normally consolidated' or virgin compressed clay. At a particular depth let the vertical effective pressure due to the overburden be σ'_v and the horizontal effective

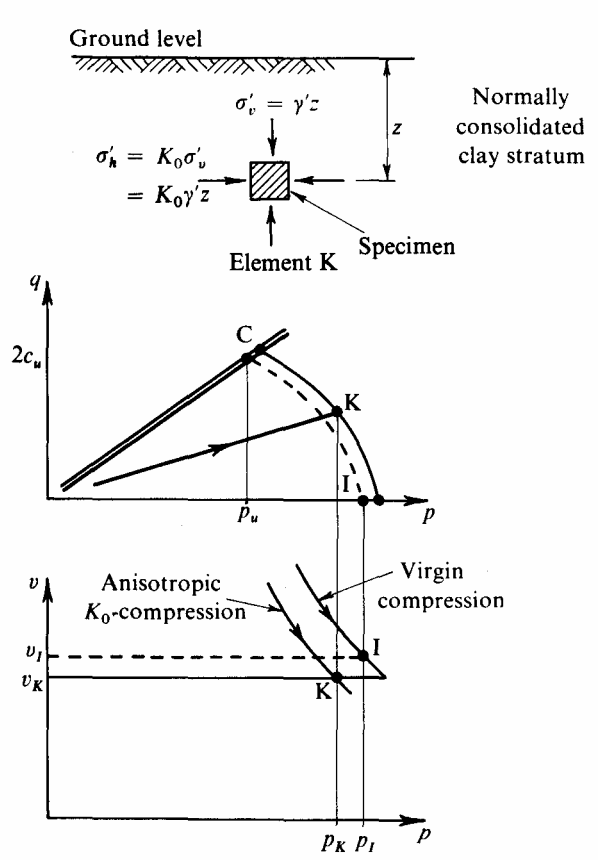

Fig. 6.17 Specific Volumes of Anisotropically Compressed Specimens

pressure be $\sigma'_h = K_0\sigma'_v$ so that the state of the specimen before extraction is represented by point K in Fig. 6.17, where

$$p_K = \frac{\sigma'_v + 2\sigma'_h}{3} = \frac{\sigma'_v}{3}(1 + 2K_0) \qquad \text{and} \qquad q_K = \sigma'_v - \sigma'_h = \sigma'_v(1 - K_0)$$

From eq. (6.20) the specific volume of the specimen v_K is given by

$$v_K = -\lambda \ln p_K + (\lambda - \kappa)\left(1 - \frac{\eta_K}{M}\right) + \Gamma$$

$$= -\lambda \ln \frac{\sigma'_v(1 + 2K_0)}{3} + (\lambda - \kappa)\left(1 - \frac{3(1 - K_0)}{M(1 + 2K_0)}\right) + \Gamma \qquad (6.41)$$

It will prove helpful to compare this specimen with an imaginary one which has been isotropically virgin compressed under the *same* vertical effective pressure $p = \sigma'_v$, so that its state is represented by point I. Its specific volume will be given by putting $K_0 = 1$ in eq. (6.41) or directly from eq. (6.20)

$$v_I = -\lambda \ln \sigma'_v + (\lambda - \kappa) + \Gamma$$

The difference in specific volume of the two specimens will be

$$v_I - v_K = \lambda \ln\left(\frac{1 + 2K_0}{3}\right) + \frac{(\lambda - \kappa)}{M}\frac{3(1 - K_0)}{1 + 2K_0}$$

$$= \lambda\left\{\ln\left(\frac{1 + 2K_0}{3}\right) + \frac{3\Lambda(1 - K_0)}{M(1 + 2K_0)}\right\} \qquad (6.41)$$

The value of Λ appears to be approximately $\frac{2}{3}M$ for most clays, so that for specimens with a minimum value of K_0 of 0.6, say, the maximum value of

$$v_I - v_K \cong \lambda\left(\ln\frac{2.2}{3} + \frac{2 \times 0.4}{2.2}\right) = \lambda(-0.3075 + 0.364) = 0.0565\lambda \qquad (6.43)$$

which even for kaolin with λ as high as 0.26 is equivalent to a difference in specific volume of only 0.0147 or only $\frac{1}{2}$ per cent water content.

Therefore, in relation to the accuracy of the unconfined compression test and this analysis we can ignore this small difference in specific volume and assume that both specimens I and K have the same v_0, and hence will be expected to reach the *same* value of c_u in a test. But we have a simple relation for the isotropically compressed sample I between its initial effective spherical pressure p_I and its final value p_u at the critical state, given by eq. (6.28)

$$\frac{p_I}{p_u} = \exp \Lambda$$

Hence, the unconfined compressive strength of both specimens is

$$2c_u = q_u = Mp_u = Mp_I \exp(-\Lambda) = M\sigma'_v \exp(-\Lambda)$$

and we have arrived at a very simple expression for the ratio of unconfined shear strength to overburden pressure of a 'normally consolidated' specimen as a *constant* for any one soil:

$$\frac{c_u}{\sigma'_v} = \tfrac{1}{2}M \exp(-\Lambda) \qquad (6.44)$$

This agrees with Casagrande's working hypothesis[13] which led to the well-established result that undrained shear strength increases linearly with depth for a 'normally consolidated' deposit. If we adopt numerical values for Weald clay of $M \cong 0.95$ and $\Lambda \cong 0.628$ this gives

$$\frac{c_u}{\sigma'_v} = 0.254$$

which agrees well with the figure of 0.27 quoted by Skempton and Sowa[14].

This result is also in general agreement with the empirical relationship presented by Skempton[15] between c_u/σ'_v (denoted as c_u/p by him) and plasticity index reproduced in Fig. 6.18, and represented by the straight line

$$\frac{c_u}{\sigma'_v} = 0.11 + 0.37\text{PI} \tag{6.45}$$

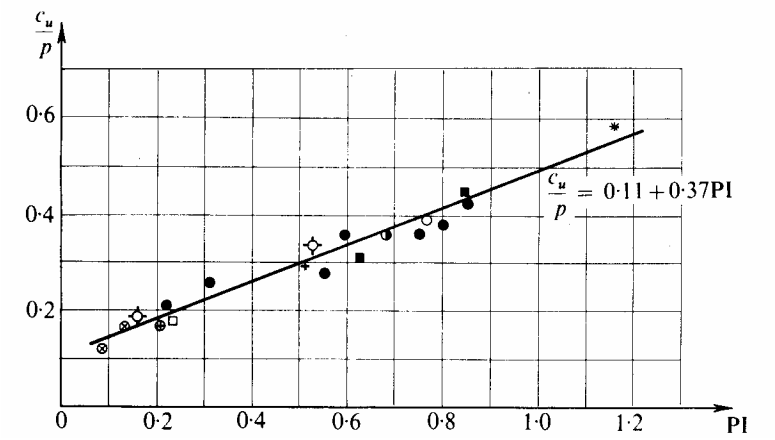

Fig. 6.18 Relationship between *cjp* and Plasticity Index for Normally Consolidated Clays (After Skempton)

If we adopt this we can use it in conjunction with eq. (6.44) to obtain another relationship between soil properties

$$M \cong (0.22 + 0.74\text{PI})\exp\Lambda \cong (0.22 + 1.267\lambda)\exp\Lambda$$

6.11 Summary

In summarizing this chapter we are aware of the point at which we decided not to introduce at this stage further theoretical developments of the critical state models. We have not introduced the generalization of the stress parameters p and q that turns eq. (6.17) into a function $F=0$ and following Mises' method of eq. (2.13) can be used to derive general plastic strain rates, but we will introduce this in appendix C. We have not introduced a research modification of the Cam-clay model that generates a corner that is less sharp for virgin compression, and shifts one-dimensional consolidation to correspond more closely with observed coefficients of lateral soil pressure. At §6.8 we called a halt to further theoretical developments, and introduced the simplified *critical state model.* With this model we have been able to interpret the simple index tests which engineers have always rightly regarded as highly significant in practice[16] but which have not previously been considered so significant in theory. In the next chapter we consider the precise interpretation of the best axial-test data and will begin by describing the sort of test for which this interpretation is possible.

References to Chapter 6

1 Roscoe, K. H. and Schofield, A. N. Mechanical Behaviour of an Idealised Wet Clay', *Proc. 2nd European Conf Soil Mech.,* pp *47 – 54 ,* 1963.

2 Roscoe, K. H., Schofield, A. N. and Thurairajah, A. Yielding of Clays in States Wetter than Critical, *Geotechnique* 13, 211 – 240, 1963.

[3] Burland, J. B. Correspondence on 'The Yielding and Dilation of Clay', *Géotechnique* 15, 211 – 214, 1965.
[4] Roscoe, K. H., Schofield, A. N. and Wroth, C. P. On the Yielding of Soils, *Géotechnique* 8, 22 – 53, 1958.
[5] Henkel, D. J. Correspondence on 'On the Yielding of Soils', *Géotechnique* 8, 134 – 136, 1958.
[6] Bishop, A. W., Webb, D. L. and Lewin, P. I. Undisturbed Samples of London Clay from the Ashford Common Shaft: Strength Effective Stress Relationships, *Géotechnique* 15, 1 – 31, 1965.
[7] Wright, P. J. F. Comments on an Indirect Tensile Test on Concrete Cylinders, *Mag. of Concrete Research 7,* 87 – 96, 1955.
[8] Skempton, A. W. and Northey, R. D. The Sensitivity of Clays, *Géotechnique* 3, 30 – 53, 1953.
[9] Skempton, A. W. Soil Mechanics in Relation to Geology, *Proc. Yorkshire Geol. Soc.* 29, 33 – 62, 1953.
[10] Casagrande, A. Classification and Identification of Soils, *Proc. A.S.C.E.,* 73, 783 – 810, 1947.
[11] Skempton, A. W. Notes on the Compressibility of Clays, *.1. Geol. Soc.,* 100, 119 – 135, 1944.
[12] Casagrande, A. Characteristics of Cohesionless Soils affecting the Stability of Slopes and Earth Fills, *J. Boston Soc. Civ. Eng.,* pp 257 – 276, 1936.
[13] Rutledge, P. C. *Progess Report on Triaxial Shear Research,* Waterways Experiment Station, pp 68 – 104, 1947.
[14] Skempton, A. W. and Sowa, V. A. The Behaviour of Saturated Clays during Sampling and Testing, *Geotechnique* 13, 269 – 290, 1963.
[15] Skempton, A. W. Discussion on the 'Planning and Design of the New Hong Kong Airport', *Proc. Inst. Civ. Eng. 7,* 306, 1957.
[16] Casagrande, A. Research on the Atterburg Limits of Soils, *Public Roads* 13, 121 – 136, 1932.